High-Performance Organic Photodetectors with Buffer Layers Suitable for In-Cell Fingerprint-Sensing Display

Xiaokang Zhou, Xingxing Chen**, Hajime Yamaguchi**, Shuning Wang, Houchi Zhang**, Xiaowei Xu**, Kunjing Zhong**, Haifeng Lu**, Rubo Xing***

***Kunshan New Flat Panel Display Technology Center Co., Ltd., Kunshan, Jiangsu, China**

**** Visionox Technology Inc., Langfang, Hebei, China**

Abstract

In this paper, we investigated the impact of OLED common layers on the performance OPDs and proposed two interfacial buffer layers, which simultaneously boost the EQE by 87-folds and suppress the dark current density by a factor of two. The introduced buffer layers are compatible with different EBLs and HBL/ETL materials, namely the buffer layers are universal. Besides, a prototype fingerprint recognition display sensor is demonstrated.

Keywords

Organic photodector (OPD), buffer layer, in-cell fingerprint recognition, health monitoring, Organic light emitting diode (OLED), image scanner

1. Introduction

Nowadays, AMOLED has been widely used in smart phones, wearables, tablets and TVs. Thinner and higher functional integration has become the trend for small and median size display application, especially for smart phones. Fingerprint recognition based on organic photodetectors (OPDs) has attracted more and more attention due to its advantages of high integration within OLED panel and ability of multi-fingerprint and palmprint recognition, as well as health monitoring [1-4].

OPD is a light sensor based on organic light sensitive materials, which absorb OLED light emission reflected by the finger and convert it to electronic signal, thus realizing the collection of fingerprint information. External quantum efficiency (EQE) and dark current density (J_{dark}) are the two primary parameters for OPDs used in fingerprint recognition, which correspond to the strength of electronic signal and noise level, respectively. Over the decades, OPD has caught up or even surpassed its inorganic counterparts in performance parameters such as EQE, J_{dark}, spectral range or normalized detectivity (D*) [5].

At present, the light emitting parts in most of AMOLED panels are fabricated by a vacuum evaporation technique, and the schematic device structure is given in Figure 1. In this technique, costly fine metal mask (FMM) with either R, G or B pixel aperture open is used to deposit the electronic blocking layer (EBL) and emitting layer (EML) for R, G and B pixel respectively, thus realizing the colorization. On the other hand, relatively low cost common metal mask (CMM) with an aperture similar to the size of AMOLED panel is used to deposit the common functional layers for all pixels, such as hole injection layer (HIL), hole transport layer (HTL), hole blocking layer (HBL), as well as all other upper layers. When integrated with OLED side by side in the fingerprint recognition application, the OPD pixel has to share the common function layers of RGB OLEDs, in order to reduce the process complexity and cost, as shown in Figure 1.

Nevertheless, the mismatch between the energy levels of functional layers in OLED and OPD, might degrade the performance of OPD, even disable the fingerprint recognition functionality [1, 6]. Therefore, it is necessary to develop new OPD donor/acceptor materials, which match well the energy levels of common layers of OLED or introduce new structures, such as interfacial buffer layers to minimize the interfacial energy barrier. Kim et. al developed a new donor and acceptor material sets to match the energy level of OLED common layers, and they found that both the energy and mobility of donor and acceptor materials are important to improve the device performance [1]. In spite of this, the mismatch between OPD materials and OLED common layers remains to be a risk when the OLED material set upgrading every one to two years. On the other hand, the buffer layers compatible with different OLED material sets will increase the flexibility in choice of both the OPD and OLED materials.

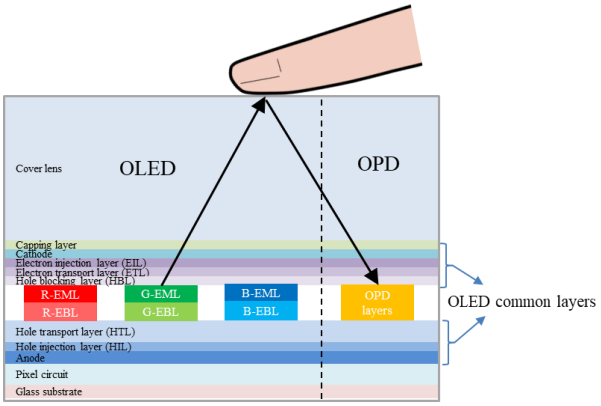

Figure 1. Schematic device structure of OLED and OPD in an in-cell fingerprint recognition sensor

In this work, based on the analysis of the energy barriers in the OPD device, we proposed and verified a series of interface buffer layers. The result shows that the p doped HTL buffer layer for the OLED HTL/OPD interface and the double buffer layer for OPD/OLED HBL interface largely reduce the energy barrier and improve the EQE and J_{dark} significantly. As demonstrated, the optimized interfacial layers function well when the EBL and HBL/ETL energy level varies over a large range.

2. Experimental results and discussion

2.1 Influence of OLED common layers on OPD performance

Firstly, OPDs both with (A1) and without (A2) OLED common layers were made to verify the influence of OLED common layers on the performance of OPD, as shown in Figure 2 (a). DM1 and AM1 are chosen as the donor and acceptor materials respectively because of their high absorption coefficient in visible light region and relatively high conversion efficiency. Besides, the HTL material for OLED is used as EBL in device A1, to suppress the dark current injection from the anode, due to its shallow LUMO level. The EQE and typical dark current density characteristics are given in Figure 2 (b) and (c). The device without OLED common layers shows an EQE of 42.4% (the values of EQE and J_{dark} represent the median value of 12 devices if not specified) at 590 nm, under -3V bias voltage, while device with OLED common layers shows much lower EQE of 0.41% and which suggests poor extraction efficiency of photogenetrated holes and electrons. Besides, the dark current density also drops and from 1.0 $\mu A/cm^2$ to 42.1 nA/cm^2, indicating hindered charge injection and transportation.

ISSN 0097-996X/25/5602-1097-$1.00 © 2025

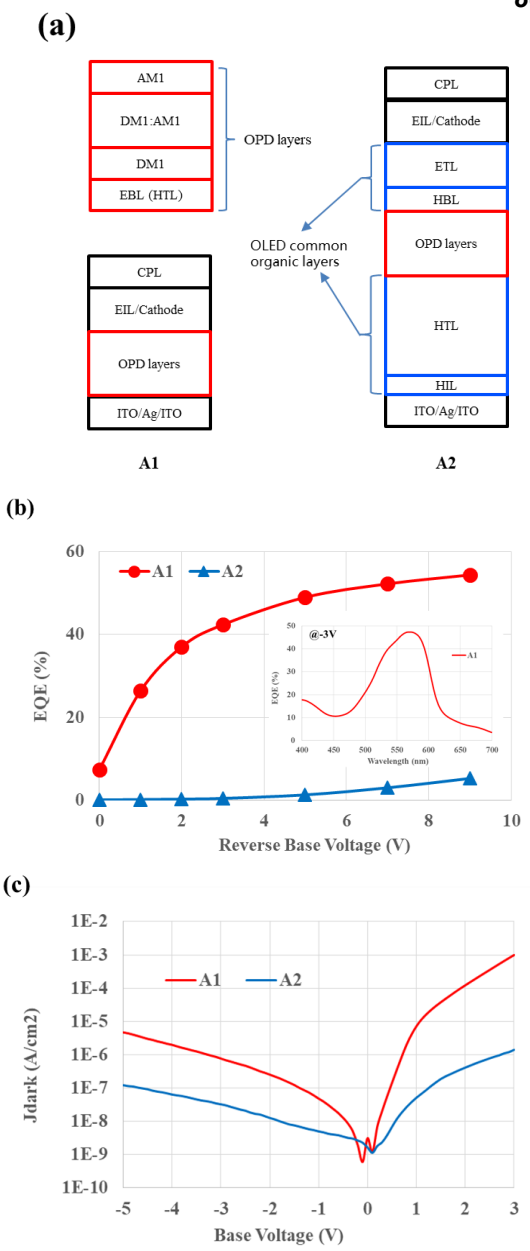

Figure 2. a) Schematic device structures of A1 and A2, b) the EQE of at 590 nm under different reverse bias voltage, the insert gives the typical spectral EQE of A1, c) typical dark current density characteristics of A1 and A2

2.2 Proposal of introduction of buffer layers

In order to figure out the underlying mechanism for the poor performance, the energy levels of materials used in device A2 are measured. As depicted in Figure 3 (a), the energy barrier is as large as 1.0 eV at the acceptor/HBL interface. While the energy difference between HOMO levels of HTL and donor is only 0.2 eV, it is found that thicker HTL leads to lower EQE and charge extraction efficiency (no shown here). Generally, the HTL in a second-order microcavity top emitting OLED is thicker than 100 nm, much thicker than the general EBLs for organic photodetectors [7]. It is suspected that, the thick HTL might either enlarge the gap due to energy realignment or enlarge the resistance due to regional charge depletion. Both the two aspects will reduce the internal electric field, which drives the charge extraction process. It is necessary to introduce interfacial buffers to minimize the energy barrier, thus improving the device performance.

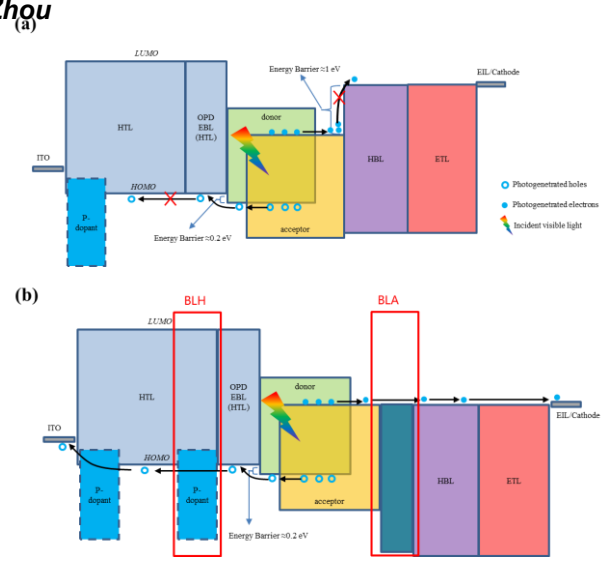

Figure 3. Schematic energy diagram of device with a) and without b) interfacial buffer layers

2.3 Buffer layer at the HTL/EBL interface (BLH)

In AMOLED a thin layer of p-doped HTL, namely the hole injection layer (HIL), is employed to improve hole injection by minimize the energy barrier between ITO and HTL. Here, device A3 is fabricated with the same device structure as A2, except for a thin layer HIL (BLH) inserted between the common HTL and OPD's EBL. As shown in Figure 4, despite the EQE of device A3 is about 10-times higher than that of A2, the EQE of A3 is still very low. In order to clarify the effect of BLH further, device A4 is made lacking of common layer of HBL and ETL compared to A3. As is shown, the EQE of device A4 increases to 57.7% at 3V reverse bias, even higher than device A1, and the EQE reaches saturation at 9V bias.

The extraction efficiency can be defined as the ratio of EQE at certain bias voltage to EQE at the saturation point (9V), and it is independent of the light absorption process. As given in Table 1, the extraction efficiency of device A3 is almost the same as A1, which suggests the BLH removes the additional energy barrier or resistance caused by the thick HTL. On the other hand, comparing A3 with A4, the lower EQE and extraction efficiency of device A3 indicates the large energy barrier at the acceptor/HBL interface. It is worth mention that, by sharing the same FMM with R or G pixel, no additional FMM is needed for the BLH layer.

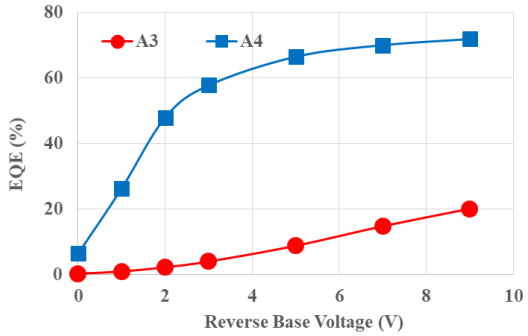

Figure 4. EQE of A3 and A4 under different reverse bias voltage (590 nm)

Table 1. Device performance of device A1 to A4 @-3V bias

Device ID	A1	A2	A3	A4
OLED common layers	without	with	with	With only HIL/HTL
BLH	without	without	with	with
Jdark (nA/cm^2)	1003.8	42.1	39.2	202.1
EQE (%)	42.4	0.41	4.0	57.8
Extraction Efficiency (%)	77.9	7.8	19.9	80.4

2.4 Buffer layer at the acceptor/HBL interface (BLA)

In this section, two materials, BLA1 and BLA2 are selected as the BLA candidates. Firstly, devices B1 and B2 were made with BLA1 and BLA2 as the buffer layer respectively, and the device performance is given in Table 2 and Figure 5. As shown, the EQE of device B1 and B2 reaches 17.5% and 20.3% respectively, much higher than that of device A3, indicating improved electron extraction efficiency and reduced interfacial energy barrier. On the other hand, the dark current also drops by half or more.

Table 2. Device performance of device B1 to B4 @-3V bias

Device ID	B1	B2	B3	B4
BLH	with			without
BLA	BLA1	BLA2	BLA1/BLA2	
Jdark (nA/cm^2)	23.9	18.5	21.4	6.8
EQE (%)	17.5	20.3	35.7	0.48
Extraction Efficiency (%)	45.8	50.5	87.3	8.7

Despite of this, the extraction efficiency is very low under low bias voltage, as shown in Figure 5. To further improve the device performance, device B3 with a double buffer layer of BLA1/BLA2 was made. As given in Table 2, the EQE of B3 increases to 35.7% and the extraction efficiency under low bias voltage also increases significantly, without sacrifice of dark current density. It is assumed that, the double layer BLA forms Ohmic contact with both the acceptor and HBL. Comparing B3 and A2, the introduction of both BLH and BLA simultaneously boosts the EQE by 87-folds and suppress the dark current density by a factor of two.

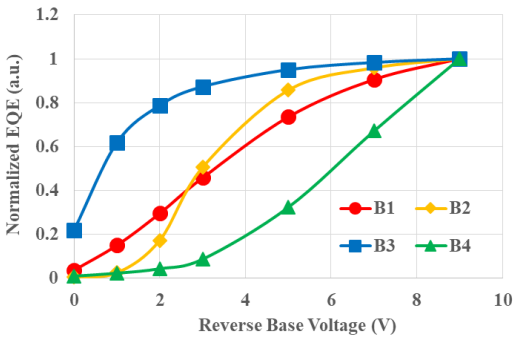

Figure 5. Extraction efficiency (normalized EQE) under different bias voltage for device B1 to B4

Further, another device (B4) with BLA only is also made. As shown in Table 2, the EQE of B4 drops to 0.48%, and the J_{dark} drops to 6.8 nA/cm^2 as well. The result suggests that, both BLH and BLA are highly necessary for the OPD with OLED common layers integrated.

2.5 Versatility of BLA and BLH

To investigate the versatility of BLH, five hole transport materials with different HOMO energy levels are tested as EBL (HTL1 is the HTL used in previous sections). As shown in Table 3, all devices show EQE>30% at -3V, suggesting efficient hole extraction at the HTL/EBL interface. Devices based on HTL 2 and HTL 3 show relative low EQE might due to the larger injection at EBL/donor interfaces. Besides, the process window of BLA is studied, and it is found that device performance keeps almost constant either the thickness or the doping ratio varies over a large range (not shown here).

Table 3. EQE and extraction efficiency of OPDs with different HTLs as EBL

EBL Materials	HTL1	HTL2	HTL3	HTL4	HTL5
ΔHOMO (eV)	0	0.3	0.4	-0.1	-0.3
EQE (%)	35.7	32.3	31.5	33.8	33.1
Extraction Efficiency (%)	87.3	81.4	84.4	87.6	86.7

To investigate the versatility of BLA, five HBL/ETL material sets are tested, which belong to different generations of OLED mass production material sets (MS1 corresponds to the HBL/ETL used in previous section). As shown in Figure 6, the extraction efficiency of different HBL/ETL sets keeps almost the same.

These results suggest that the proposed BLA and BLH are compatible with different EBL and HBL materials.

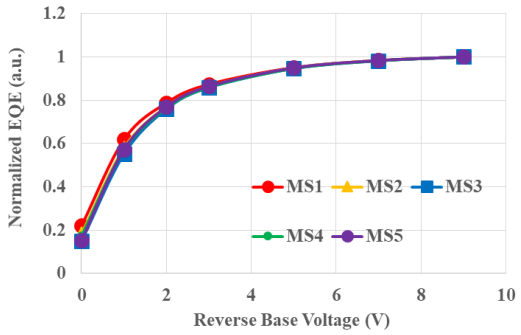

Figure 6. Extraction efficiency (normalized EQE) for OPDs with different HBL/ETL material sets

2.6 Origin of dark current

Device B4 shows much lower dark current than device A2 and B3, which means the introduction of BLA lowers the J_{dark}, while the BLH will increase the J_{dark}. In device A2, thick HTL and the injection barrier cause a large resistance both in the dark and under illumination. However, at the acceptor/HBL interface, dark current might generate via the interfacial traps, thus device A2 shows a relative high J_{dark}. The inset of the BLA passivates the interfacial trap and leads to lower dark current in B4. On the other hand, the use of BLH will lower the resistance caused by thick HTL and increase both dark current and photocurrent. It is worth mention that, another origin of dark current is metal penetration (during thermal evaporation) caused shorts, as the devices based on Mg:Ag cathode show higher dark current than those base on Al cathode (not shown here).

2.7 Device lifetime

To characterize the lifetime of OPDs, devices with BLH and BLA are aged in a homemade aging equipment with constant green light illumination (~1 mW/cm^2) and bias voltage of -3V. The EQE is measured after aging for a certain interval of time. As given in Figure 7, the EQE keeps higher than 90% after 1000 hours operation. A much longer lifetime is expected with an accelerated aging condition at the initial stage, for example ten times stronger light illumination.

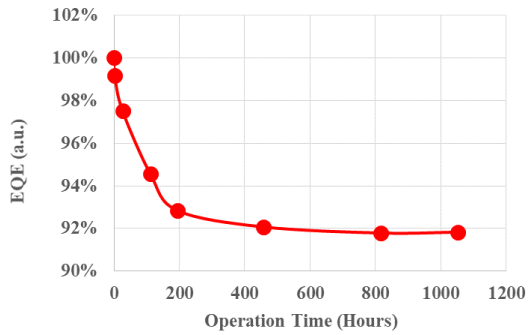

Figure 7. The measured EQE with extended aging time

3. Demonstration of fingerprint recognition display sensor

Base on the proposed device structure, a fingerprint recognition display sensor is fabricated. Due to the lack of optical shielding structure (black matrix) and electric isolation structure (separator), the optical and electric crosstalk are strong enough to cover the fingerprint information. For demonstration, a fingerprint pattern with a width of 1 cm is printed on paper and the image of the fingerprint pattern is collected by the sensor under external illumination. As shown in Figure 8 (b), the collected fingerprint image reproduces most of the features in the original image. On the other hand, the OLED functions well and Figure 8 (c) gives the image of display sensor panel with green light on.

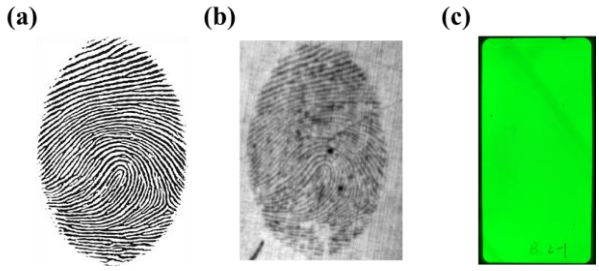

Figure 8. a) The fingerprint pattern, b) the collected fingerprint pattern image, c) the image of display sensor panel with green light on

4. Conclusions

In this work, high performance organic photodetector for in-cell fingerprint recognition application is realized by the introduction of interfacial buffer layers, which reduces energy barriers between OPD layers and OLED common layers. Both buffer layers at the HTL/OPD interface and the acceptor/HBL interface are compatible with different OLED functional material. We believe that our work would bring new sights into the R&D of organic photodetectors.

References

1. Kim, S., Yoon, S., Kim, S.W., Choi, M.-S., Kim, H., Lee, D.-Y., Moon, S. and Park, K.-B. (2023), 54-2: Invited Paper: Novel Display Application beyond OLED: All-in-one Sensor Display. SID Symposium Digest of Technical Papers, 54: 782-784..
2. Bae, K.S., Kim, G.H., Park, H.A., Park, J., Ahn, T., Lee, D., Moon, S., Kim, J., Kim, C. and Kim, Y. (2024), 13-3: Full Screen Fingerprint Display with Embedded Organic Photo-detectors. SID Symposium Digest of Technical Papers, 55: 142-145.
3. Kim, S., Yoon, S., Jung, J., Choi, M.-S. and Kim, C. (2024), 13-1: Invited Paper: New Frontier in Display Technology: OPD Sensor in OLEDs for Healthcare Application. SID Symposium Digest of Technical Papers, 55: 136-137.
4. Kamada, T., Niikura, Y., Hatsumi, R., Oishi, A., Watanabe, K., Sugimoto, K., Kubota, D., Yamagata, S. and Yamazaki, S. (2024), 13-4: OLED/Organic Photodetector Dual-Mode Device Integrated into Side-by-Side Patterned OLED Display. SID Symposium Digest of Technical Papers, 55: 146-149.
5. Yang, D., & Ma, D. (2018). Development of Organic Semiconductor Photodetectors: From Mechanism to Applications. Advanced Optical Materials, 1800522.
6. Wang, J., Li, R., Tian, H., Juan, A., Zuo, P., Chen, S., Liu, Z. and Shi, S. (2023), P-128: Characteristic optimization method of organic photodetector based on OLED integrated backplane. SID Symposium Digest of Technical Papers, 54: 1326-1329.
7. Zhou, X., Yang, D. and Ma, D. (2015), Extremely Low Dark Current, High Responsivity, All-Polymer Photodetectors with Spectral Response from 300 nm to 1000 nm. Advanced Optical Materials, 3: 1570-1576.